

Fuel Saving Assessment from a Simulated Hybrid Photovoltaic-Diesel System Using Forecasts-Integrated Control from a Sky Imager

Louis-Étienne Boudreault, Olivier Liandrat, Jean Pottier, Étienne Buessler, Sylvain Cros, Nicolas Schmutz
Reuniwatt, 14 rue de la Guadeloupe, 97490 Sainte-Clotilde, France

Abstract—Fuel savings opportunities from forecast integration into the controls of a hybrid 4MWp PV and 12.5MW diesel system are assessed from plant control simulations. The forecasts are performed using the *SkyCam Vision*, a ground-based sky imager observing clouds and providing solar irradiance forecasts used to make decisions on the ignition control of the gensets. Real PV production, load and forecast historical data were extracted from the plant and were used as inputs to a hybrid system simulator for performing genset control. Scenarios with diesel only, a baseline case without forecasts and an ideal forecast case are also simulated for comparison. The results show fuel economy of 5k\$/year by using the *SkyCam Vision* forecasts as compared to the baseline scenario, while improving the management of difficult PV drop events from cloud anticipation. The *SkyCam Vision* proves a safe and cheap solution for bringing further operation costs reductions into hybrid projects.

I. INTRODUCTION

Hybrid photovoltaic-diesel systems are becoming increasingly popular within the current shift towards electrification of isolated and remote communities [1]. Such systems proved useful at regions where interconnection to the existing grids is too expensive or not possible, as well as to meet the energy requirements by means of a cost-effective solution.

A thermal plant alone with diesel generators can be considered for such projects, but is exposed to various risks related to fuel transportation towards these remote areas (loss, theft, geopolitical context, etc.). In an evolving background where diesel-market prices are also uncertain, the current trend is to shift toward a reduction of reliance on fossil fuels. Meanwhile a solar plant alone would involve lower operation costs, it does not guarantee itself a safe integration into the grid due to the variability of the solar resource powering the photovoltaic (PV) production at the frontend. Combined together, PV energy reduces the costs while diesel compensates the PV variability risk.

Various management strategies exist as to always provide the needed load when a sudden drop in solar resource occurs within hybrid PV-diesel systems. One approach is to bring an excessive number of gensets online so as to always provide enough power at any time, when needed. However, this strategy of oversizing the spinning reserve has the disadvantage of causing many of the gensets to run at a minimum shared load, typically around 30-40% of their nominal power, leaving the gensets in a state of suboptimal fuel consumption due to a lower efficiency at low power-load. Another alternative is to include a storage device such as a battery to store the excess PV energy during favorable

weather and to release this energy to compensate any fluctuating power deficit that may occur. In this case, the diesel generators only serves as an eventual side backup to cover the rest of the needed demand for example during night-time operation or during harsh weather conditions. A drawback of this approach is that the prices of battery systems are currently prohibitive, hardly making such hybrid project competitive in terms of costs compared to other solutions, however this situation is expected to rapidly change in the future [2]. A third approach implies a careful management of the gensets' spinning reserve, where the generators are switched off when appropriate and brought back online only when needed. This approach has the advantages of lowering the overall fuel consumption by optimizing the spinning reserve, but may however expose the power plant at risks to critical power deficits when the spinning reserve is not sufficient to absorb severe PV drops. In such management approach, sky imagers can play a key role to optimize further the spinning reserve while allowing for improved grid stability by bringing online in due time the gensets only when the clouds abruptly change the PV production. Such solution is already on-the-shelf, while sky imagers are also expected to play an important optimization role within the future trends in energy storage.

A few simulation analysis exist where different scenarios are compared together to seek for an optimal configuration and sizing of a hybrid PV-diesel system [3], [4], often performed using the software HOMER [5]. However, fewer focused on the control of the system itself to improve its efficiency (see e.g. [6], for review), and forecast integration has only being investigated up to very recently [7].

The purpose of this study is to quantify the economical benefits of using the *SkyCam Vision* sky imager to perform hybrid PV-diesel plant control through genset start/stop scheduling. For this task, a new hybrid PV-diesel system simulator was designed internally at Reuniwatt, the *hybrid-Cast* code. Actual load and PV production data together with on-site historical forecasts were extracted from an actual site located in Oiapoque, Brazil, and served as input to the simulator.

The paper is structured as follows. Section II first describes the site, the *SkyCam Vision* forecasting system and the control methodology defined within the hybrid simulator and with the different case scenarios simulated. In section III, outputs from the simulations are processed and discussed. We finally move to section IV where the costs implications of the simulations are analysed and a brief conclusion is provided in section V.

II. METHODOLOGY

A. Hybrid PV-diesel plant simulated

The hybrid PV-diesel power plant simulated powers mostly a residential-type load and is located on an isolated grid near the border of French Guiana in Oiapoque, Brazil. It consists in,

- A 3.3MWp capacity PV power plant and,
- A 12.5MW capacity thermal plant where the gensets are assumed being 10 identical 1250kW diesel generators.

The actual load and PV production data were extracted from the site to perform the following simulations. The period investigated was between 2019-01-05 and 2019-01-14, making a total of 10 consecutive days. The peak load reaches a maximum of 6000kW around september-october for this grid and about 5000kW during the period of investigation, mainly occurring around 19:00 local time.

B. The SkyCam Vision

The *SkyCam Vision* is a camera system used by the *InstaCast* firmware, which provides forecasts every 30 seconds from whole-sky images acquired in the visible waveband using a fisheye lens. The camera sensor is set in a high-definition range (HDR) mode to construct a fused image from intermediate images at different exposure times. The resulting image shows enhanced contrasts and illuminations of cloud scenes as compared to cameras with no HDR mode. The camera includes a global horizontal irradiance (GHI) sensor used as a “truth” measurement basis to perform the forecasts. The camera also includes an onboard mini-PC together with a data storage device to perform a local processing of the images. The forecasts are communicated directly over the local network of the power plant to the energy management system (EMS) through Modbus TCP/IP protocol.

The basic principle of *InstaCast* is to predict forward in time the GHI time series recorded from the sensor at each time-step. To perform this task, a multi-step procedure is applied. First, a calibration is performed where each pixels are attributed zenith-azimuth angles following the position of the sun. Second, Random Forest Regressors [9] are trained each day on a serie of inputs based on a combination of both image and dynamical features. The image features include cloud fraction and the dynamical features, a serie of image sections containing the cloud cover status traced-back from the sun position at various time-horizons from a single motion vector calculated with an optical flow algorithm [8]. The latter motion vector is calculated using two consecutive images, at a 30 seconds interval.

Here, the 30 seconds forecasts produced at the end of this chain are resampled to 1 minute and an empiric linear model for converting GHI into power is applied.

C. Hybrid PV-diesel system control

The general power balance $B(t)$ of the hybrid PV-diesel system is described as the following,

$$B(t) = \underbrace{P_{PV}(t)}_{\text{PV plant}} + \underbrace{P_{gen,tot}(t)}_{\text{Thermal plant}} - \underbrace{L(t)}_{\text{Load}}, \quad (1)$$



(a)



(b)

Fig. 1. (a) The *SkyCam Vision* camera system at the Oiapoque site in Brazil and (b) a related snapshot extraction of the sky vault.

where $B(t)$ should be zero at every instant if enough power is provided to the system by the PV and thermal plants to compensate the load. In this study, the produced P_{PV} is always considered at 100% of its output, meaning that no curtailment is applied to the PV. The remaining power is provided by the gensets' and their overall power target setpoint is set as,

$$P_{setpoint}(t) = L(t) - P_{PV}(t). \quad (2)$$

We then search trough all k gensets ready and running in a fixed order ($k = 1..10$) as $P_{gen,tot} = \sum_{k=1}^k P_{gen,k}(t)$, and note the minimum $k_{min} = k$ where the available power exceed the setpoint $P_{gen,tot} > P_{setpoint}$. Then, all gensets where $k \leq k_{min}$ are set to 100% of their capacity ($= P_{gen,nom}$) while the actual genset ($k = k_{min}$) is adjusted so that,

$$P_{gen,k_{min}} = \left(\sum_{k=1}^{k_{min}} P_{gen,k} \right) - P_{setpoint}. \quad (3)$$

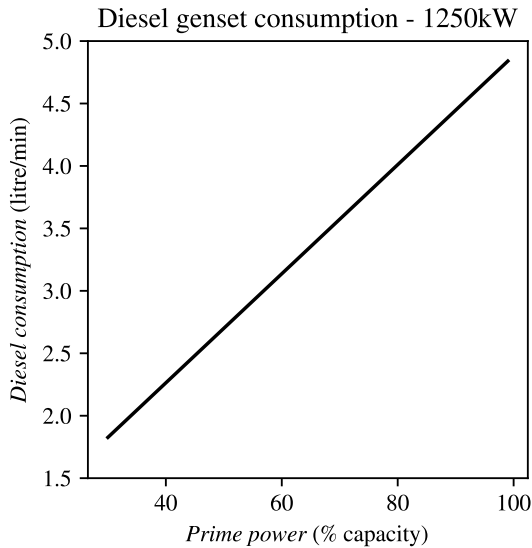


Fig. 2. Consumption curve of the 1250kW diesel generators simulated. The curve shows that 2 generators running at 50% of their capacities will consume more (5.4l/min) than a single genset running at 100% of its capacity (4.9l/min). Extracted from datasheet provided by Voltaia.

This process is repeated at every time step. Note that the gensets are run in a so-called asymmetric load sharing mode, meaning that the total load is shared between the gensets such that the first ignited gensets run at 100% of their capacities while the last ignited genset varies as the remaining load only¹. This operation mode is meant to optimize the overall fuel consumption of the thermal plant as the efficiency of a single generator is higher when the load applied is close to its nominal power, as seen with the consumption curve of the diesel generators shown in Fig. 2.

A successful power balance depends whether a sufficient number of gensets were brought online over the previous time-steps. The decisions to either switch on or switch off a given genset depends on the control scenario considered, which are explained in the next section. Before making these decisions for any such control case, the following conditions must first be satisfied,

- After being switched on, a genset has a spin-up time of 2 minutes before any load can be applied ($T_{start} = 2\text{mins}$).
- Before being switched off, a genset must be operated for a minimum runtime of 30 minutes ($T_{stop} = 30\text{mins}$).
- A genset can only be run as low as 30% of its nominal output ($P_{gen,min} = 375\text{kW}$).

The minimum runtime condition aims at avoiding untimely switching off of the gensets and the minimum power condition to prevent any “wet stacking”² effects, which would both make the gensets operate beyond their safe operation

¹For example, for a needed load of $L = 3000\text{kW}$, the two first gensets will provide $P_{gen,1} = 1250\text{kW}$ and $P_{gen,2} = 1250\text{kW}$, respectively, while only the last ignited genset will provide the rest of the needed load, i.e. $P_{gen,3} = 500\text{kW}$

²Wet stacking is an effect where the engine cylinders do not reach efficient combustion and results into some unburned fuel cycling towards the exhaust system.

range, possibly resulting into hasty maintenances.

D. Genset ignition/extinction control rules

In this study, four control scenarios are compared, namely a *diesel only* control case and three hybrid PV-diesel control cases implying different ignition management rules. The latter include a *Baseline* no-forecast case, an *Ideal forecasts* case and a *SkyCam Vision* case. For any of these cases, the decision of starting or stopping a genset is performed for the so-called *next priority genset*, with the decision based on the actual genset for which the power setpoint calculated makes it run at partial load ($< 100\%$). The extinction criterion is identical for all cases and is stated as:

The next priority genset is stopped when the load on the actual genset goes below 70% of its nominal power output, i.e. $P_{gen,k,min} < 0.70 \times P_{gen,nom} = 875\text{kW}$.

The ignition criterion differs amongst the cases and are described below.

1) *Diesel only case:* The *diesel only* case assumes no PV, only the thermal plant is used to provide the load balance (hence $P_{PV}(t) = 0$ at all times). The ignition rule is defined as:

The next priority genset is switched on if the load on the actual genset goes beyond 80% of its nominal power output, i.e. when $P_{gen,k,min} > 0.80 \times P_{gen,nom} = 1000\text{kW}$.

2) *Baseline case:* The *Baseline* case follows the exact same ignition rule as for the *Diesel only* case, except that all the power produced by the PV plant is used when calculating the load balance setpoint in Eq. 2. This scenario represent standard hybrid plant control where no forecasts are used.

3) *Ideal forecast case:* The *Ideal forecasts* case is an hypothetical reference case as if the future PV production was exactly known for igniting the gensets. In this scenario, the next priority genset is switched on according to the worst forecasted PV drop ΔP in the next 2 minutes as,

$$\Delta P(t) = P_{gen,k,min} - \min(P_{PV}(t_d)), \quad (4)$$

where P_{PV} are the forecasted power values within $t_d \in [t, t+2\text{mins}]$. Then, the next priority genset is, if not already, switched on when either one or the other following criterion is satisfied:

$$\Delta P(t) > 0.5 \times P_{gen,nom}, \quad (5)$$

$$P_{gen,k,min} > 0.99 \times P_{gen,nom} = 1237\text{kW}. \quad (6)$$

The first criterion serves as igniting the gensets based on the significant forecasted PV drops while the second criterion serves as smooth transition for calling for additional spinning reserve when no significant drop are forecasted ahead, for example during night-time operation. The coefficients in Eqs. 5 and 6 (0.5 and 0.99) were adjusted based on fuel consumption and grid stability optimization.

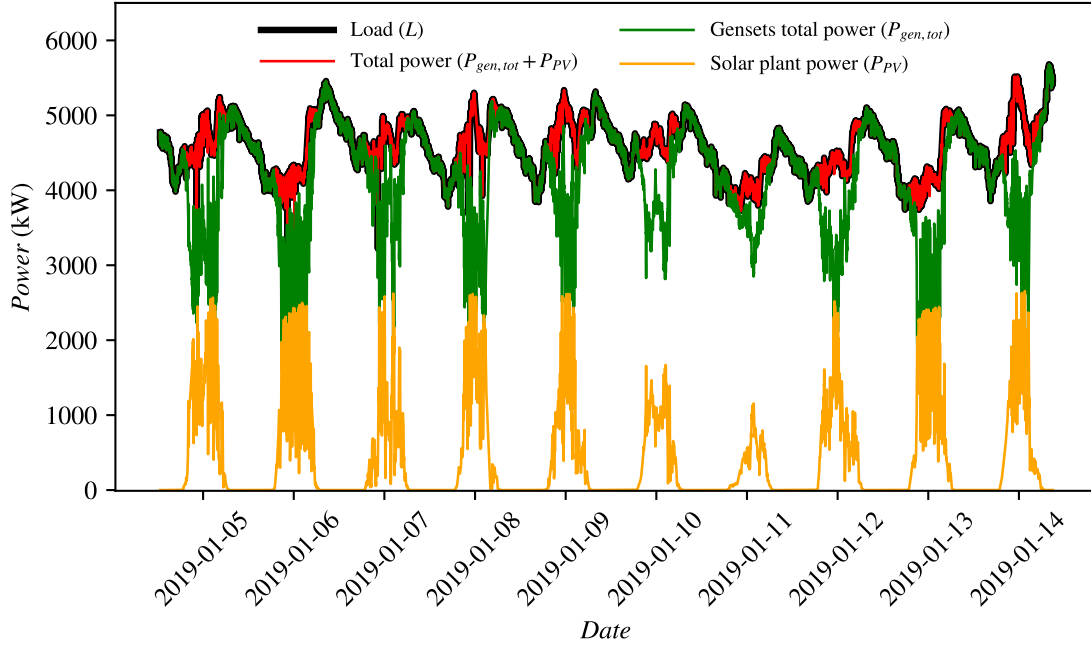


Fig. 3. Simulated time series of the load and the load share between the PV plant and the thermal plant for the *SkyCam Vision* control case.

4) *SkyCam Vision* case: The *SkyCam Vision* case uses the real forecasts performed at the site with the sky imager to predict the future PV power output and make a decision on the next priority genset ignition. As for the *Ideal forecast* case, we look ahead at the 2 minute PV forecasts such that the minimum ΔP drops are calculated,

$$\Delta P(t) = P_{gen,k_{min}} - \min(P_{PV}(t_d) - \varepsilon_{PV}(t_d)). \quad (7)$$

with $t_d \in [t, t + 2mins]$. Similarly, the next priority genset is ignited when either one or the other criterion is satisfied:

$$\Delta P(t) > 0.6 \times P_{gen,nom}, \quad (8)$$

$$P_{gen,k_{min}} > 0.99 \times P_{gen,nom} = 1237kW. \quad (9)$$

$\varepsilon_{PV}(t)$ is here a safety error correction function aiming at compensating the errors made with the sky imager on the forecasted power, here defined as a linear ramp as,

$$\varepsilon_{PV}(t_d) = C_\varepsilon \times t_d, \quad (10)$$

where $C_\varepsilon = 240kW/min$ is a coefficient taken here as 7%/min (relative to the PV peak power being 3300kWp). As for the *Ideal forecast* case, the coefficients (0.6 and 0.99) along with C_ε were optimized according to optimal fuel consumption and grid stability considerations. An in-depth error analysis of the forecasting system is currently undergoing to design a better optimized error function than the above ramp function [10].

III. RESULTS

The power time series for the *SkyCam Vision* case are shown for the full period in Fig. 3. The genset total power curve (in green) in this figure is resulting from grid control simulations based on the load and PV production. The load generally follows a general tendency where a low peak occurs around 5:00 during night-time and high peak near 17:00 in the evening, typical of a residential consumption

curve. The PV output shows typical PV production curve in relation to the sun's path, with the peak power reaching around 2.5MW about midday, superimposed with strong power variability caused by clouds passing. In this isolated grid without any other power stations, the gensets' power completes the difference between the load and the PV power.

The load share is better seen in Fig. 4 for the specific day of 2019-01-05. The green curve in the uppermost graph shows the total genset production summed together whereas the individual genset productions are shown in the separate lowermost graphs. For this day, only the first 5 gensets are sufficient to provide the needed power. The first genset (DG1) produces most of the time at 100% power, with some lower production occurring when large fast ramping up occurs (see e.g., between 13:00-15:00). The second to fourth gensets (DG2 to DG4) show more fluctuating load, with DG3 becoming completely extinct between 11:00 and 13:00. DG5 shows little load variability, suggesting that this generator only serves as spinning reserve when needed, especially when night-time production is needed and starts about the peak load near 17:00. DG4 and DG5 show many small 30 minutes period operating at minimum power (30%), where an immediate genset start is followed by a genset stop. The strongest PV drops are occurring near after 13:00 and 14:00. In the case of the near-after 13:00 drop, it is seen that the camera forecasts has called DG5 in operation just in time to absorb this strong drop event while DG3 was switched off. Similarly, for the near-after 14:00 PV drop event, DG4 was brought online right on time by the camera for absorbing this strong drop.

All control cases scenarios detailed in Section II-D are now compared in Table I. The total genset energy $E_{gen,tot} = \frac{\Delta t}{60} \sum_{t=0}^{\infty} P_{gen,tot}(t)$ is unexpectedly higher for both the *Ideal forecast* and *SkyCam Vision* cases as compared with the *Baseline* case. This is explained by the fact that the *Baseline* scenario involves more underproduction situations

2019-01-05

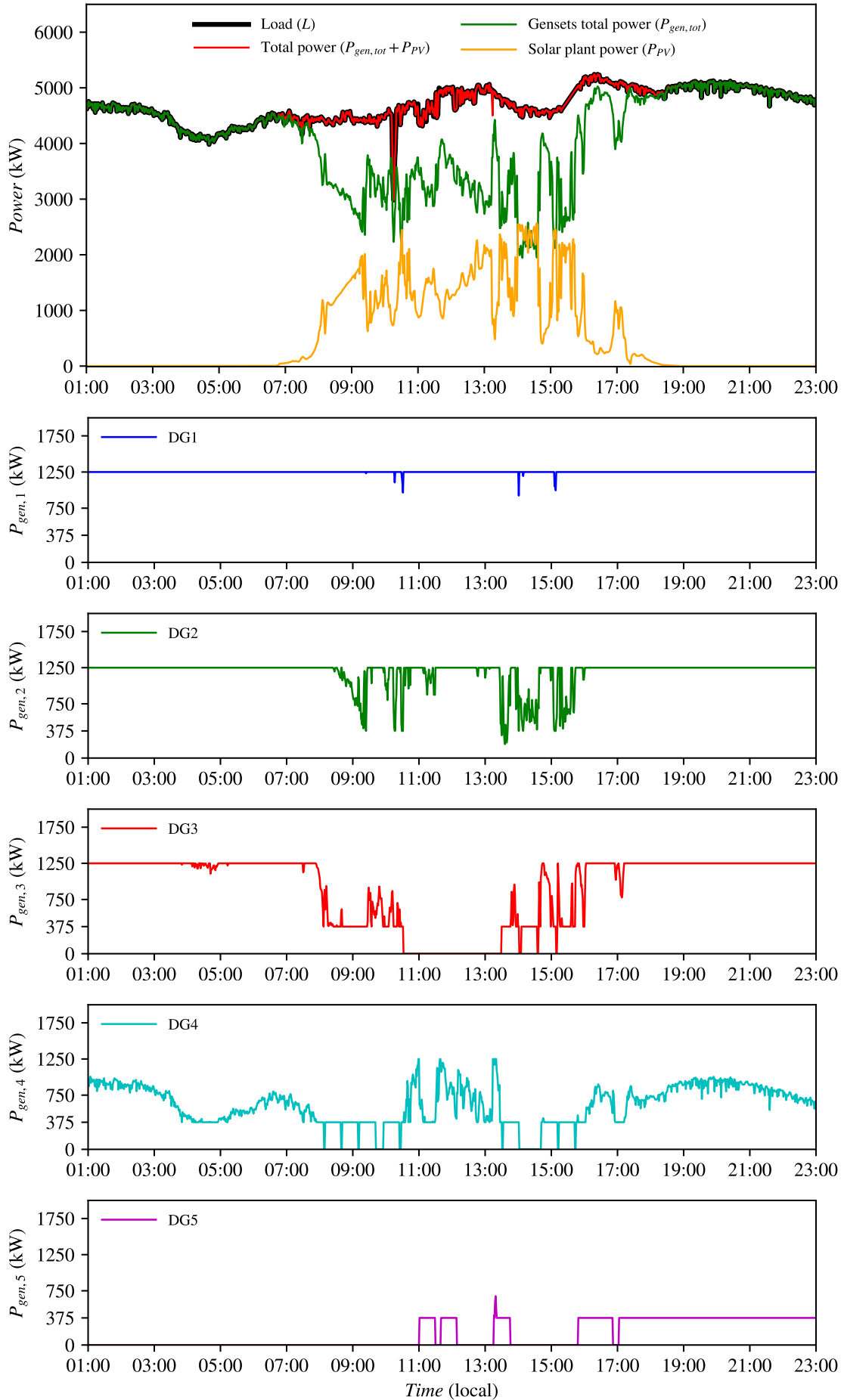


Fig. 4. Simulated hybrid PV-diesel system power balance (uppermost figure) along with individual diesel gensets (DG) power output (lower figures) for the SkyCam Vision control case.

TABLE
TOTAL ENERGY AND DIESEL CONSUMPTIONS FOR THE VARIC

Control case	Diesel only	Baseline
Total genset energy (kWh)	1 085 618	984 000
Total PV energy (kWh)	0	100 000
Spinning reserve (%)	11.46	17.5
Diesel litres consumed (l)	259 968	236 000
Max genset overload (%)	120	110

with potential blackouts, where the total produced power by the gensets cannot fully balance the load, making the total consumed energy lower. Such situations happen when the 80% load criterion for calling additional spinning reserve does not leave enough time to absorb the steep PV drops (not shown). The most critical underproduction event would make the gensets run on overload, at 135% of their capacity (see the Max genset overload³, Table I). For Oiapoque, the load trip setting is set to 114% with a maximum overload duration of < 5mins tolerated (DEIF, personal communication). This would make the *Diesel only* and *Baseline* case involve at least one simulated blackout during the period of investigation. The simulated blackouts would completely be avoided as concerns the *Ideal forecast* and *SkyCam Vision* cases, for which the max genset overload calculated are 112% and 113%, respectively, with durations of < 2mins. Note that the *Ideal forecast* case imply overload situations due to periods where a generator become suddenly extinct together with a PV drop occurring at the same time (not shown). Such event could be prevented further by adjusting the extinction criterion according to forecoming PV drops.

Overall, the results indicate that the spinning reserves⁴ are both reduced for the *Ideal* and *SkyCam Vision* forecast-control scenarios as compared to the *Baseline* management scenario, by 0.05% and 0.01% respectively. This spinning reserve reduction translates respectively into 672 litres and 132 litres of fuel savings over the 10 days considered, representing about 24 900 litres and 4890 litres of fuel savings when reported over a full year. Note that the diesel litre consumption is obtained from the power conversion of the individual gensets summed together using the consumption curve shown in Fig. 2. The *Diesel only* case involves the lowest spinning reserve, which is explained by the fact that the scenarios involving PV are calling for more spinning reserve to absorb the PV drops. The consequences of these results are discussed in the next section.

IV. DISCUSSION

To compare the costs that the various scenarios would imply over a normal operation year, the yearly operation costs of the thermal plant are presented side-by-side for the various scenarios in the barplot shown in Fig. 5. These calculations are performed for a constant diesel fuel price of 0.9\$/l. For illustration, the costs of PV is also added on top of the fuel consumption costs, assuming a PV price

³The maximum genset overload (%) corresponds to the situation where the load deficit $B(t)$ redistributed among the k running gensets at that specific time make the gensets run at a certain percentage higher than their nominal capacity (i.e. > 100%).

⁴The spinning reserve (%) is here calculated as the energy difference between the total available genset energy relative to the total consumed genset energy, i.e. $SR = \frac{\Delta E}{E_{tot}} \sum_{t=0}^{\infty} (1 - P_{gen,tot} / P_{gen,tot,avail}) \times 100$.

of
e)
of
th
W
oj
st
w
7;
th
th
P
pl
th
ac
Ir
oi
sz
P
m

in
g;
fc

il
s
n
r.
y
l
n
,
r
s
e
l
n
,
r.
-
a
e
o

d
r
s
s

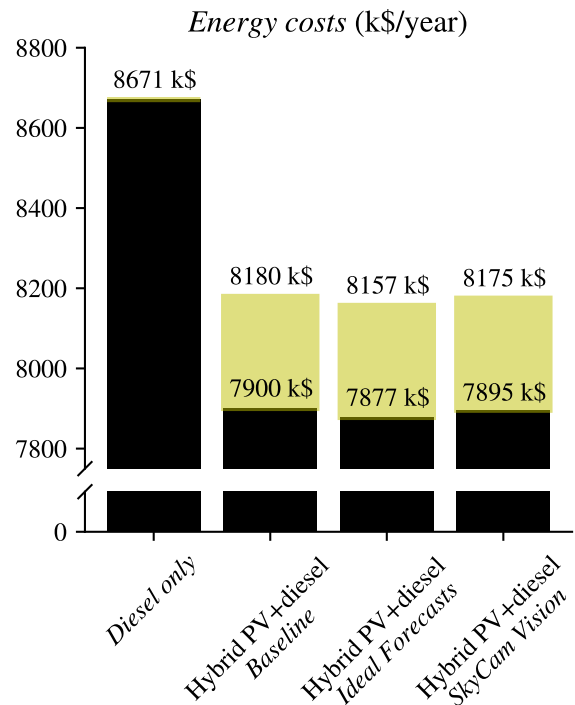


Fig. 5. Energy costs for the various control cases. The black portions of the bars represent the diesel consumption costs and the yellow portion the overall costs of PV. A price of 0.9\$/l is assumed for diesel and a price of 0.075\$/kWh for PV.

that further fuel savings as far as 22k\$/year are possible by bringing improvements to the forecasting system (compared to current gains of 5k\$/year). We believe that using a more advanced forecasting system, such as for instance the *Sky Insight* [11], which is based on a thermal-infrared camera, could potentially bring savings to a scale closer to the *Ideal forecast* case in terms of these operation costs. Note that only the ignition control of the gensets was performed with the forecasts in this study. Further optimizations could be reached by adjusting, for example, the extinction criterion according to forecasts. In this case, the forecasts could help predict the forecoming clearsky events and forestall the next priority genset extinction, thereby bringing further optimization to the spinning reserve when no clouds are seen ahead. This type of optimization will be investigated in a further study.

V. CONCLUSION

Simulations of a hybrid PV-diesel power plant in Brazil were performed to evaluate the benefits of forecast-integrated control using the *SkyCam Vision* sky imager. Actual load, PV production and forecast data were used as input to the simulations to perform the genset control of the plant. Various control scenarios were then reproduced, where the gensets are started either using a fixed threshold dependent on the load or by using forecasts according to future PV drops information. Results indicated that the *SkyCam Vision* allows for further fuel economy when compared to a baseline hybrid PV-diesel scenario using no forecasts, while improving the plant control safety. Overall, the study showed that forecasts-integrated control can be safely and cheaply considered for bringing higher cost-efficiency to hybrid PV-diesel projects.

REFERENCES

- [1] B. Wichert *PV-diesel hybrid energy systems for remote area power generation A review of current practice and future developments*. Renewable and Sustainable Energy Reviews, 1(3):209–228, 1997.
- [2] S. Ericson, K. Anderson, J. Engel-Cox, H. Jayaswal, D. Arent, *Power couples: The synergy value of battery-generator hybrids*. The Electricity Journal, 31(1):51–56, 2018.
- [3] D. Yamegueu, Y. Azoumaha, X. Py and N. Zongoa *Experimental study of electricity generation by Solar PV/diesel hybrid systems without battery storage for off-grid areas*. Renewable Energy, 36(6):1780–1787, 2011.
- [4] M. Usman, M. Tauseef Khan, A. Singh Rana and S. Ali *Techno-economic analysis of hybrid solar-diesel-grid connected power generation system*. J. Electr. Syst. Inform. Technol., 5(3):653–662, 2018.
- [5] HOMER official webpage <www.HOMERenergy.com>
- [6] A. Mohammed, J. Pasupuleti, T. Khatib, W. Elmenreich, *A review of process and operational system control of hybrid photovoltaic/diesel generator systems*. Renewable and Sustainable Energy Reviews, 12(1):436–446, 2015.
- [7] D. Peters, T. Kilper, M. Calais, T. Jamal and K. von Maydell *Solar short-term forecasts for predictive control of battery storage capacities in remote PV-diesel networks*. In: Transition Towards 100% Renewable Energy, Springer International Publishing, Chapter 29: 325–333, 2018.
- [8] G. Farneback, *Two-Frame Motion Estimation Based on Polynomial Expansion*. In: Proceedings of the 13th Scandinavian conference on Image analysis. Josef Bigun and Tomas Gustavsson (Eds.). Springer-Verlag, Berlin, Heidelberg, 2003. pp. 363–370.
- [9] L. Breiman, *Random forests*. Machine Learning, 45(1):5–32, 2001.
- [10] L.-E. Boudreault, F. Kurzrock, O. Liandrat, G. Roussel, E. Buessler and S. Cros, *Performance evaluation metrics for very short-term PV forecasting*. In: European Geosciences Union (EGU) General Assembly 2019, Vienna, Austria, 7–12 April 2019.
- [11] O. Liandrat, S. Cros, A. Braun, L. Saint-Antonin, J. Decroix, L. and N. Schmutz, *Cloud cover forecast from a ground-based all sky infrared thermal camera*. In: Proceedings Volume 10424 - Remote Sensing of Clouds and the Atmosphere XXII, p.104240B, 2017.